Journal of Crystal Growth 401 (2014) 279–284

Contents lists available at ScienceDirect

Journal of Crystal Growth

journal homepage: www.elsevier.com/locate/jcrysgro

Formation of ZnO rods with varying diameters from ε-$Zn(OH)_2$

Jing Wang, Lan Xiang*

Department of Chemical Engineering, Tsinghua University, Beijing 10084, China

ARTICLE INFO

Available online 16 February 2014

Keywords:
A1. Nanostructures
A1. Crystal morphology
B1. Nanorods
B1. Zinc oxide
B2. Semiconducting II–VI material

ABSTRACT

The influence of temperature on the formation of one-dimensional (1D) ZnO from ε-$Zn(OH)_2$ via solution route was studied in this paper, using $ZnSO_4$ and NaOH as the raw materials. The experimental results indicated that the increase of temperature from 25 °C to 80 °C accelerated the conversion of ε-$Zn(OH)_2$ to ZnO, leading to the formation of 1D ZnO with comparative big diameters. A two-stage route was then developed to synthesize ZnO nanorods with diameters of 20–100 nm and lengths of 1–3 μm by aging $Zn(OH)_2$ in 1.0 mol L^{-1} NaOH at 25 °C for 72 h followed by aging the slurry at 80 °C for 2 h. Compared with the ZnO submicron-rods (diameters: 100–500 nm, lengths: 1–3 μm) formed at 80 °C, the ZnO nanorods formed via the two-stage route exhibited a thinner diameter and a higher photo-degradation activity for Rhodamine B owing to the pre-formation of ZnO nanorods (diameters: 10–50 nm) on ε-$Zn(OH)_2$ surface at 25 °C as well as the existence of more oxygen defects.

1. Introduction

The controllable synthesis of one-dimensional (1D) ZnO nanomaterials has been widely studied in recent years owing to their unique electronic/optoelectronic properties and potential applications in nanoscale electronics or photonic devices, catalysts and ceramics, etc. [1–4]. ZnO nanorods with small diameters were usually used for the fabrication of gas sensors, field emission devices, solar cells and the photo-catalysts, etc. [4–7] owing to their distinctive geometries and size effects. Many methods have been developed to synthesize ZnO nanorods such as chemical vapor deposition, electrochemical deposition, sol–gel and aqueous solution method, etc. [8–11], specially, the aqueous solution method has attracted much attention owing to the moderate conditions and the easy control of ZnO properties.

The former aqueous solution synthesis of ZnO nanorods were difficult to be scaled-up since they were usually carried out in dilute solutions. For example, Morin et al. produced ZnO nanowires with diameters of about 22 nm and lengths up to 10 μm in 3×10^{-6} mol L^{-1} $Zn(NO_3)_2$ solution [12]. Liu et al. [13] synthesized the ZnO nanorods with diameters of 10–30 nm and lengths of about 1 μm at room temperature from the solution containing 0.03–0.05 mol L^{-1} $Zn(NO_3)_2$ and 1.0 mol L^{-1} NaOH. The surfactant-assisted routes were usually employed to adjust the diameters of ZnO nanorods. For example, Qiu et al. reported that the presence of 0.008–0.01 moL L^{-1} polyethylenimine (PEI) decreased the diameters of 1D ZnO from 250 nm to 100 nm [14]. Li et al. synthesized ZnO nanowires with diameters of 30–50 nm and lengths of 2 μm by hydrothermal treatment of the $Zn(OH)_4^{2-}$ solution at 140 °C for 24 h in the presence of polyethylene glycol (PEG400) [15].

Recently, increasing attention has been paid to the solution growth of 1D ZnO from ε-$Zn(OH)_2$ precursor owing to the moderate conditions, the high efficiency and the capability for scaling-up [16–23]. For example, Mcbride et al. [16] reported the formation of ZnO micro-rods with an average diameter of 1 μm and lengths up to 9.5 μm from ε-$Zn(OH)_2$ in 0.375 mol L^{-1} NaOH at 101 °C; Wang et al. [21] fabricated the micro-flowers composed of ZnO needles with diameters of 100–300 nm and lengths of 3–5 μm from ε-$Zn(OH)_2$ in 1.60 mol L^{-1} NaOH at 80 °C for 10 h; Li et al. [17] developed a SDS-assisted method to produce ZnO submicro-rods with diameters of 450–550 nm and lengths of 15 μm in 1.0 mol L^{-1} NaOH at 80 °C. It was noticed that the former work only reported the formation of ZnO rods with diameters in micro- or submicron-scale from ε-$Zn(OH)_2$, the fabrication of ZnO nanorods was still a challenge.

Herein, a facile solution method was developed to synthesize ZnO rods with varying diameters from ε-$Zn(OH)_2$ precursor. The influence of temperature on the formation of ZnO rods was studied and a two stage route was developed to synthesize ZnO nanorods with diameters of 20–100 nm and lengths of 1–3 μm.

2. Experimental

Commercial reagents with analytical grade were used in the experiments without further purification. ε-$Zn(OH)_2$ precursor

* Corresponding author. Tel: +86 10 62788984.
E-mail address: xianglan@mail.tsinghua.edu.cn (L. Xiang).

http://dx.doi.org/10.1016/j.jcrysgro.2014.01.070
0022-0248

were prepared by drop-wise addition (3 ml min^{-1}) of 2.0 mol L^{-1} $ZnSO_4$ into 4.0 mol L^{-1} NaOH under stirring (300 rpm) at 25 °C, keeping the molar ratio of OH^- to Zn^{2+} as 2:1. The slurry containing ε-$Zn(OH)_2$ precipitate was kept stirring for 10 min, then filtrated, washed with deionized water and dried at 25 °C for 24 h. 1.50 g of ε-$Zn(OH)_2$ was dispersed in 40.0 ml of 1.0 mol L^{-1} NaOH, the slurry was kept aging at 25–80 °C for 2–72 h, the final product was filtrated, washed and dried at 60 °C for 12 h.

The morphology and microstructures of the samples were examined with a field emission scanning electron microscopy (FESEM, JSM 7401F, JEOL, Japan) and a high resolution transmission electron microscopy (HRTEM, JEM-2010, JEOL, Japan). The structures of the samples were identified by X-ray powder diffractometer (XRD, D8 Advance, Bruker, Germany) using CuKα (λ=0.154178 nm) radiation. The surface compositions of the samples were characterized by X-ray photoelectron spectrometer (XPS, PHI-5300, PHI, USA). The concentrations of soluble Zn(II) were analyzed by EDTA titration. The room temperature photoluminescence spectra were measured on a Hitachi F-7000 luminescence spectrometer using Xe lamp with an excitation wavelength of 325 nm.

The photo-catalytic activities of ZnO rods were evaluated by detecting the degradation of RhB aqueous solution containing 4 mg L^{-1} RhB and 200 mg L^{-1} ZnO under ultraviolet light irradiation originated from 16 W UV lamp. The suspensions were sampled and centrifuged every 20 min and the RhB concentrations were determined by measuring the absorption at 554 nm using an UV–vis spectrophotometer (UV-8453, Agilent, USA).

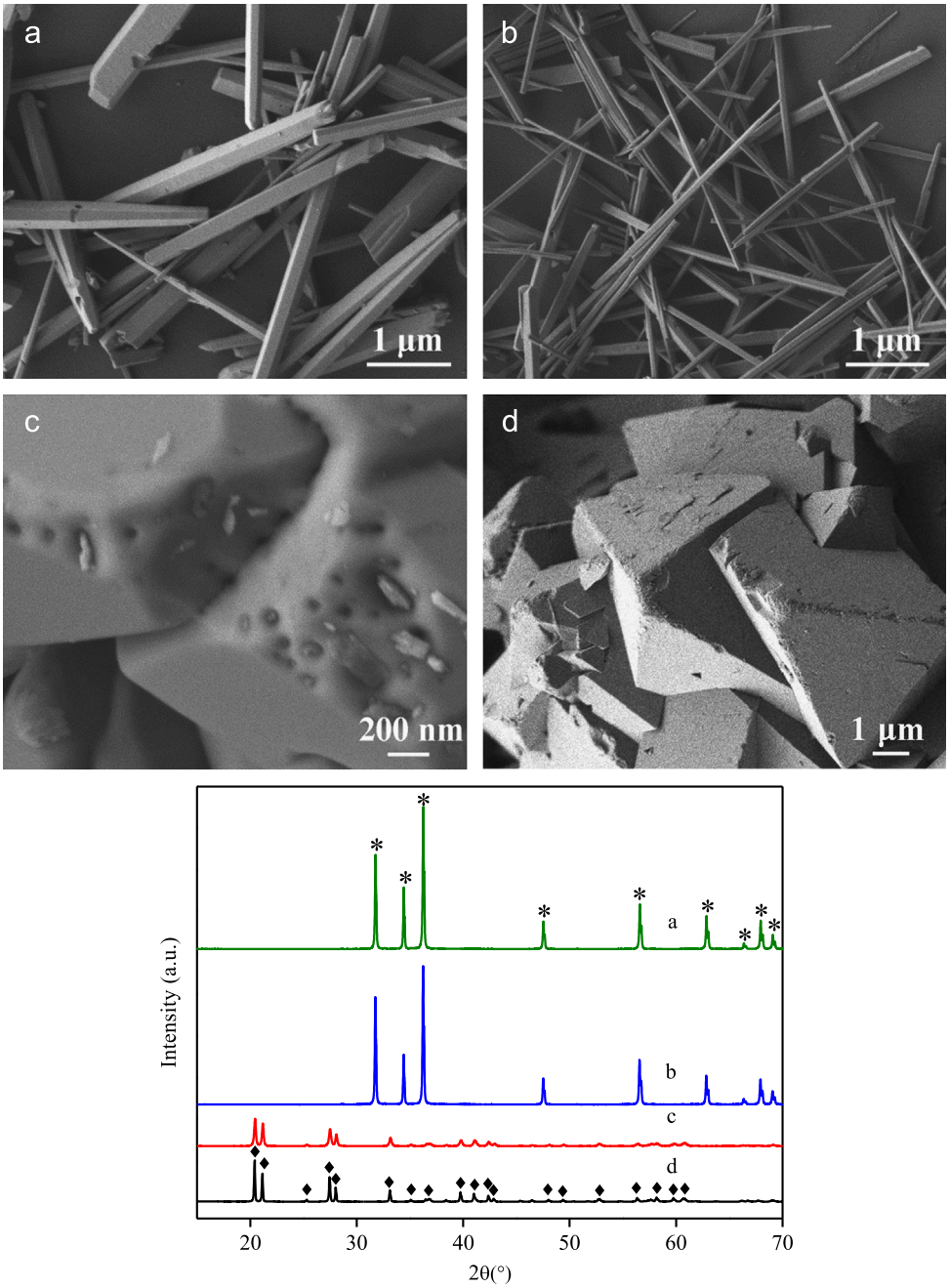

Fig. 1. Morphology and XRD patterns of the samples formed at different temperatures and time. Temperature (°C): (a) 80, (b) 60, (c and d) 25; time (h): (a) 2.0, (b)6.0, (c) 72, and (d) 0; ♦: ε-$Zn(OH)_2$, ∗: ZnO.

3. Results and discussion

3.1. Influence of temperature on the formation of ZnO rods from ε-Zn(OH)$_2$

Fig. 1 shows the morphology and XRD patterns of the samples formed at different temperatures. ZnO submicron-rods with diameters of 100–500 nm and lengths of 1–3 μm formed after aging the ε-Zn(OH)$_2$ precursor in 1.0 mol L^{-1} NaOH solution at 80 °C for 2.0 h. The time needed for complete conversion of ε-Zn(OH)$_2$ to ZnO was prolonged to 6.0 h at 60 °C and ZnO submicron-rods with diameters of 50–200 nm and lengths of 1–3 μm were obtained. Compared with ε-Zn(OH)$_2$ precursor composed mainly of the octahedral particles, the surfaces of the product formed by aging ε-Zn(OH)$_2$ at 25 °C for 72 h became cracked and pitted with some rod-like particles with diameters of 10–50 nm, implying the possible formation of a minor amount of ZnO rods at room temperature even though no XRD peaks for ZnO phase occurred. The influence of temperature on the solution growth of ZnO rods has been widely investigated previously. Li et al. [24] studied the chemical bath deposition of ZnO nanorod array at temperatures ranging from 65 °C to 95 °C and demonstrated that low temperature favored the formation of thinner nanorods. However, in their case, ZnO rods were directly precipitated from solution, not grown from ε-Zn(OH)$_2$ intermediate. Recently, Nicholas et al. [22] investigated the temperature-dependent precipitation of ε-Zn(OH)$_2$ and ZnO phase, and demonstrated that low temperature favored the formation of ε-Zn(OH)$_2$ phase, however, the influence of temperature on the growth of 1D ZnO from ε-Zn(OH)$_2$ has not been reported. In the present work, the conversion of ε-Zn(OH)$_2$ to ZnO and the anisotropic growth of ZnO rods were connected with the temperature, and the increase of temperature from 25 °C to 80 °C accelerated the formation of 1D ZnO with big diameters.

Fig. 2 shows the TEM and HRTEM images of the samples formed after aging ε-Zn(OH)$_2$ in 1.0 mol L^{-1} NaOH at 25 °C for 72 h. The HRTEM image in Fig. 2b (corresponding to the framed part of the nanorod in Fig. 2a) demonstrated that the interplanar spacing was 0.26 nm which was quite similar to that of (001) planes of ZnO, indicating the preferential growth of the ZnO nanorods along the *c*-axis.

Fig. 3 shows the O1s XPS spectra of the samples formed before (a) and after (b) aging ε-Zn(OH)$_2$ in 1.0 mol L^{-1} NaOH at 25 °C for 72 h. In the case of ε-Zn(OH)$_2$ raw material, the detected O1s spectrum for ε-Zn(OH)$_2$ occurring at 532.6 eV could be resolved to two peaks located at 533.3 eV and 531.7 eV, corresponding to the O1s binding energies of O in H$_2$O (532.9–533.3 eV [25]) and Zn–OH (531.9–531.5 eV [26]), respectively. In the case of the aged sample, the detected O1s spectrum occurring at 531.5 eV could be resolved to three peaks located at 532.9 eV (H$_2$O), 531.5 eV (Zn–OH) and 530.8 eV, respectively. The peak occurred at 530.8 eV should be assigned to the lattice oxygen in ZnO [25]. The above results reconfirmed the formation of ZnO on ε-Zn(OH)$_2$ surface after aging ε-Zn(OH)$_2$ in 1.0 mol L^{-1} NaOH at 25 °C for 72 h.

3.2. Formation mechanism of ZnO rods

The dissolution–precipitation and the in-situ crystallization mechanisms have been suggested by the former researchers to explain the formation of ZnO from ε-Zn(OH)$_2$, but the detailed

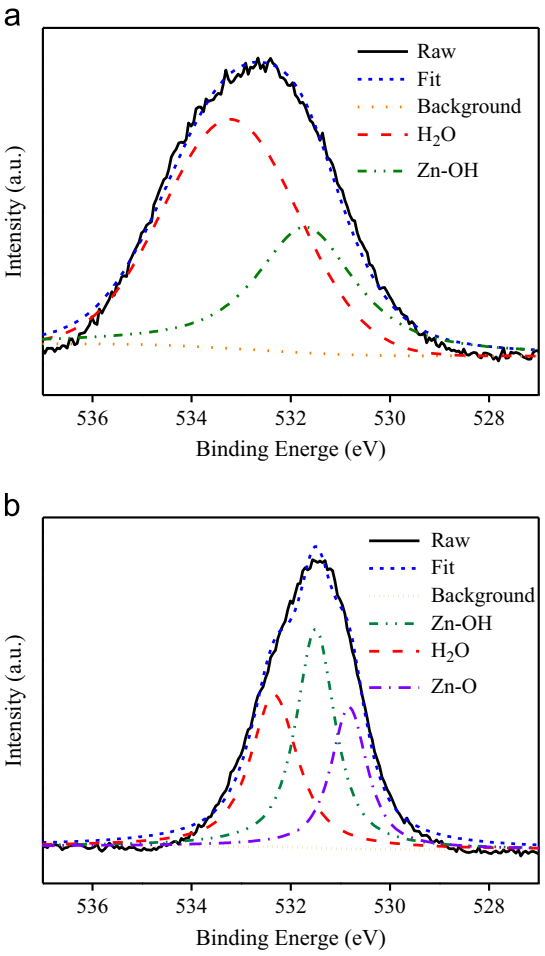

Fig. 3. O1s XPS spectra of the samples formed before (a) and after (b) aging ε-Zn(OH)$_2$ in 1.0 mol L^{-1} NaOH at 25 °C for 72 h.

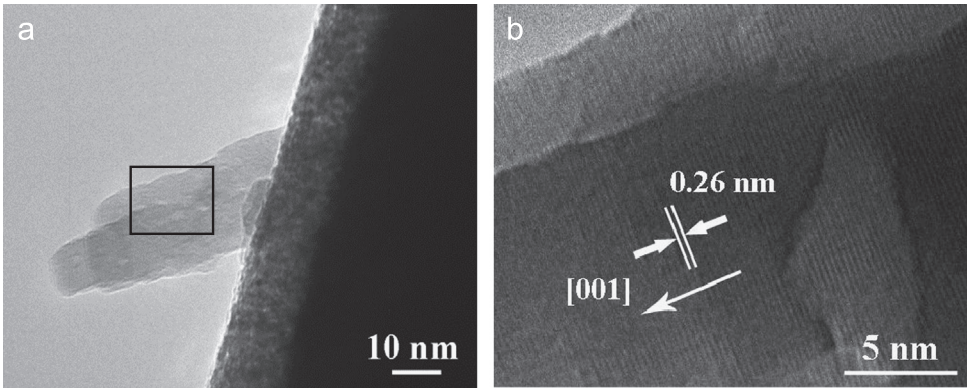

Fig. 2. TEM (a) and HRTEM (b) images of the samples formed after aging ε-Zn(OH)$_2$ in 1.0 mol L^{-1} NaOH solution at 25 °C for 72 h.

phase transformation behaviors were still unclear [18,20–22]. Fig. 4 shows the variation of soluble Zn(II) concentrations with reaction time during the aging processes of ε-$Zn(OH)_2$ in 1.0 mol L^{-1} NaOH at 25–80 °C. In the cases of 80 °C and 60 °C, the Zn(II) concentrations increased gradually in the initial time owing to the quicker dissolution of ε-$Zn(OH)_2$ than the precipitation of ZnO and decreased in the later time due to the faster formation of ZnO than the dissolution of ε-$Zn(OH)_2$, revealing the existence of the dissolution–precipitation mechanism in the phase transformation processes. In previous work, the dissolution–precipitation mechanism was often proposed based on the SEM observations [21,24] and the variation of dissolution–precipitation rates with temperature has not been considered. Here, the lower concentrations of soluble Zn(II) at 60 °C than those at 80 °C indicated the slower dissolution of ε-$Zn(OH)_2$ and the formation of ZnO at 60 °C, which favored the formation of ZnO rods with thin diameters [12]. The concentrations of soluble Zn(II) became much lower at 25 °C than those at 60–80 °C, leading to the formation of merely a minor amount of ZnO nanorods with diameters of 10–50 nm on ε-$Zn(OH)_2$ surfaces even after aging ε-$Zn(OH)_2$ in 1.0 mol L^{-1} NaOH at 25 °C for 72 h.

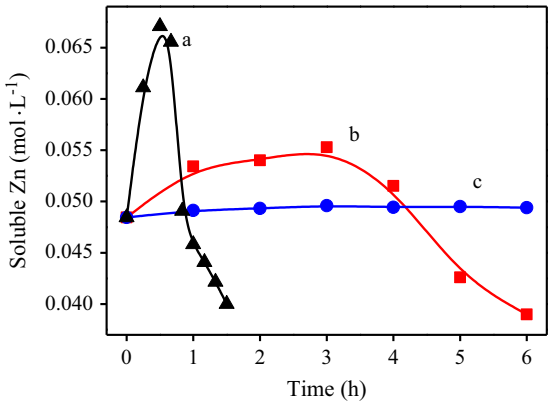

Fig. 4. Variation of soluble Zn(II) with reaction time. Temperature (°C): (a) 80, (b) 60, and (c) 25.

Fig. 5 shows the morphology of the products formed at different reaction time and temperatures. The occurrence of the small holes on ε-$Zn(OH)_2$ surface and the appearance of ZnO nanorods in some holes implied the possible in-situ crystallization route in the initial formation of ZnO. The formation of the holes should be connected mainly with the volume shrinkage in the dehydration process of ε-$Zn(OH)_2$ due to the density difference between ε-$Zn(OH)_2$ (3.1 g cm^{-3}) and ZnO (5.6 g cm^{-3}). The subsequent oriented growth of the ZnO rods outside ε-$Zn(OH)_2$ crystals should be attributed mainly to the dissolution–precipitation mechanism [21]. Thus the in-situ crystallization and dissolution–precipitation mechanisms coexisted in the present conditions, the former one dominated in the initial nucleus and growth stages and the latter one guided the subsequent oriented growth processes. It was also noticed that the prolongation of reaction time led to the slight increase of the diameters of the ZnO nanorods from 50–400 nm to 100–500 nm at 80 °C and 20–100 nm to 50–200 nm at 60 °C, indicating that the diameters of the ZnO rods were dependent mainly on the initial diameters of the ZnO formed at the beginning stage.

3.3. Formation of ZnO nanorods via two-stage route

A two-stage route was employed to synthesize ZnO nanorods with thin diameters. ε-$Zn(OH)_2$ precursor was firstly aged in 1.0 mol L^{-1} NaOH at 25 °C for 72 h to form primarily a minor amount of ZnO nanorods with small diameters (10–50 nm) on ε-$Zn(OH)_2$ surfaces, the slurry was then aged at 80 °C for 2 h to promote the quick and complete conversion of ε-$Zn(OH)_2$ to ZnO nanorods. Fig. 6 shows the SEM image, TEM and inserted HRTEM images of the ZnO nanorods prepared via the two-stage route. ZnO nanorods with diameters of 20–100 nm and lengths of 1–3 μm were synthesized via the two-stage route. The occurrence of the lattice fringes with a spacing of 0.26 nm in the HRTEM image in Fig. 6b indicated the *c*-axis oriented growth of the ZnO nanorods.

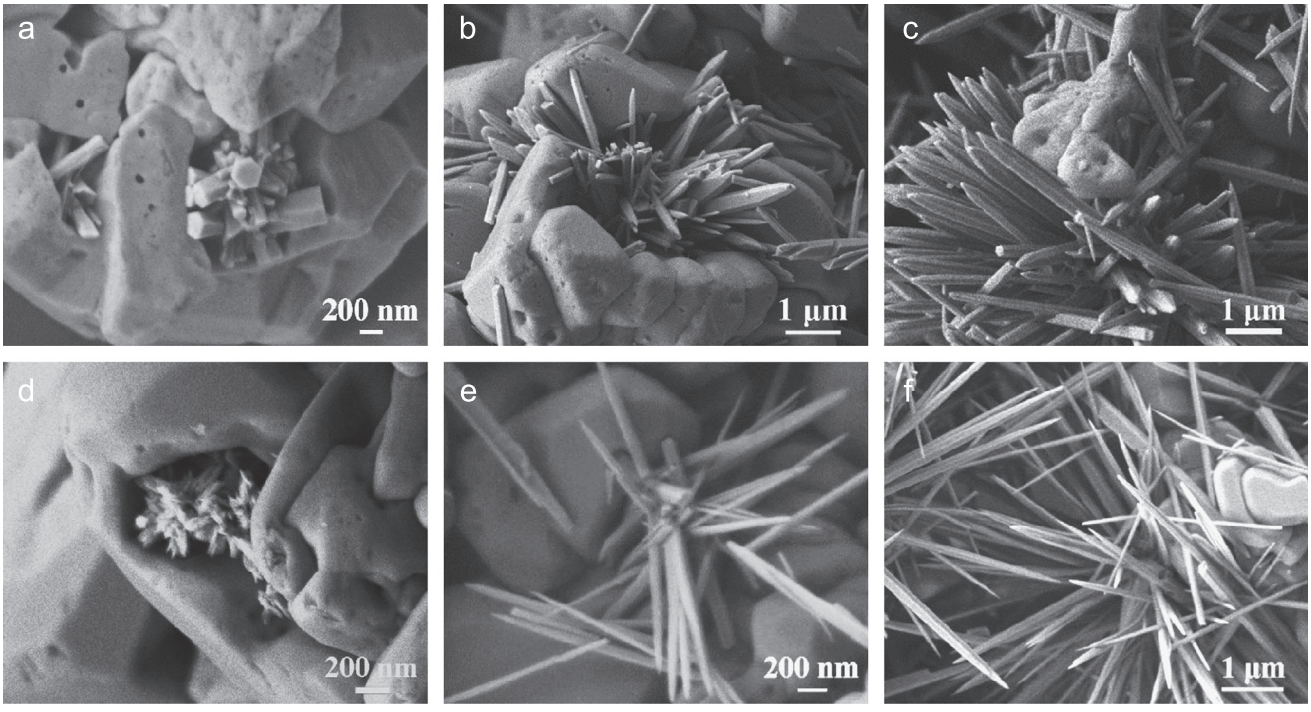

Fig. 5. Morphology of the products formed at different time and temperatures. Temperature (°C): (a–c) 80, (d–f) 60; time (h): (a) 0.25, (b) 0.5, (c) 0.67, (d) 0.5, (e) 1.0, and (f) 3.0.

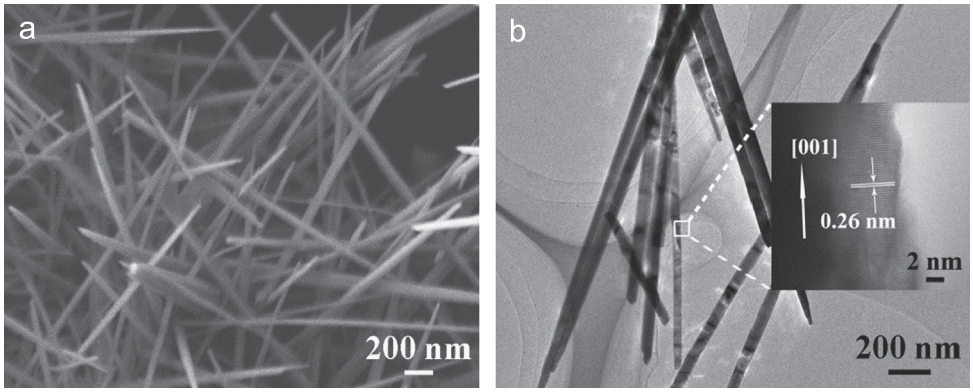

Fig. 6. SEM image (a), TEM and inserted HRTEM images (b) of ZnO nanorods prepared via two-stage route.

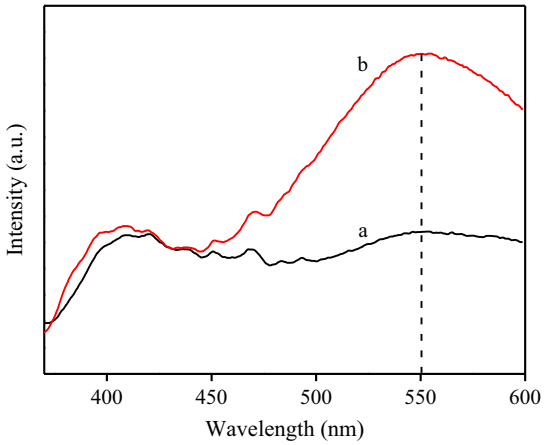

Fig. 7. Photoluminescence spectra of ZnO rods formed via one stage (a) and two-stage (b) routes.

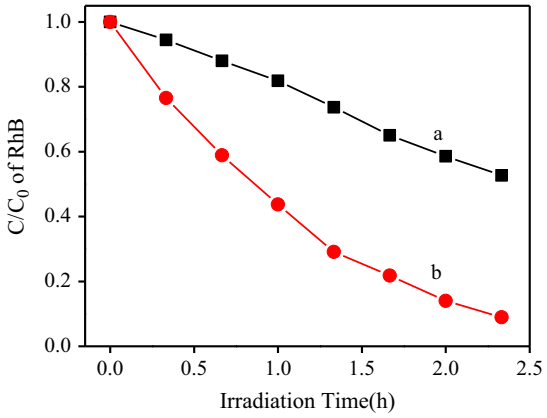

Fig. 8. Photo-degradation of RhB in the presence of ZnO rods formed via one stage route (a) and two-stage route (b).

Controlling the morphology of ZnO via two-stage route was also suggested in some former studies, but the roles of the first stage were different. Qiu et al. [27] reported the fabrication of ZnO nanorod arrays using a preheating hydrothermal process and found that the preheating stage lowered the precursor concentration which favored the formation of ultralong ZnO nanorods. Xu et al. [28] developed a two-stage hydrothermal route for synthesis of long ZnO nanowire arrays by dividing the growth process into two steps at two different temperatures to enhance the growth rate difference between crystals. In the present case, the role of the first stage is controlling the diameters of the initially formed ZnO nanorods on ε-$Zn(OH)_2$ surface.

Fig. 7 shows the photoluminescence (PL) spectra of the ZnO submicron- and nano-rods formed via the one-stage route (aging ε-$Zn(OH)_2$ in 1.0 mol L^{-1} NaOH at 80 °C for 2 h) and the two-stage route. The broad band emission peaks located at 551 nm should be attributed to the green emission originated from the surface oxygen defects of ZnO and the intensity of the green emission was proportional to the amount of the oxygen defects [29]. The stronger intensity in curve b than that in curve a indicated that compared with the ZnO submicron-rods formed via the one-stage route, the ZnO nanorods formed via the two-stage route contained more oxygen defects.

Fig. 8 shows the photo-degradation of RhB in the presence of ZnO submicron-rods formed via one stage route and ZnO nanorods formed via two-stage route. After 2.3 h of irradiation, 90% and 53% of RhB were degraded in the presence of ZnO nanorods and ZnO submicron-rods, respectively. The faster degradation of RhB in the presence of ZnO nanorods should be attributed to the existence of more oxygen defects in the ZnO nanorods, which were usually considered as the active sites of the ZnO photo-catalyst [30].

4. Conclusions

A facile two-stage route was developed to synthesize ZnO nanorods with thin diameters and high photo-degradation activity by aging ε-$Zn(OH)_2$ precursor in 1.0 mol L^{-1} NaOH at 25 °C for 72 h followed by aging of the slurry at 80 °C for 2 h. The initial formation of minor amount of ZnO nanorods with diameters of 10–50 nm on the ε-$Zn(OH)_2$ surface at 25 °C promoted the subsequent formation of ZnO nanorods with thin diameters at 80 °C. Compared with the ZnO submicron-rods formed at 80 °C, the ZnO nanorods formed via the two-stage route possessed more surface oxygen defects and enhanced photo-degradation activity.

Acknowledgments

This work was supported by the National Science Foundation of China (no. 51174125, no. 51234003 and no. 51374138) and National Hi-Tech Research and Development Program of China (863 Program, 2012AA061602).

References

[1] M.H. Huang, S. Mao, H. Feick, H. Yan, Y. Wu, H. Kind, E. Weber, R. Russo, P. Yang, Room-temperature ultraviolet nanowire nanolasers, Science 292 (2001) 1897–1899.

[2] Z.L. Wang, J. Song, Piezoelectric nanogenerators based on zinc oxide nanowire arrays, Science 312 (2006) 242–246.
[3] A. Soukiassian, A. Tagantsev, N. Setter, Anomalous dielectric peak in Mg and Li doped ZnO ceramics and thin films, Appl. Phys. Lett. 97 (2010) (Article Number 192903).
[4] J.L. Yang, S.J. An, W.I. Park, G.C. Yi, W. Choi, Photocatalysis using ZnO thin films and nanoneedles grown by metal–organic chemical vapor deposition, Adv. Mater. 16 (2004) 1661–1664.
[5] M. Law, L.E. Greene, J.C. Johnson, R. Saykally, P. Yang, Nanowire dye-sensitized solar cells, Nat. Mater. 4 (2005) 455–459.
[6] Y. Fang, Q. Pang, X. Wen, J. Wang, S. Yang, Synthesis of ultrathin ZnO nanofibers aligned on a zinc substrate, Small 2 (2006) 612–615.
[7] Y. Huang, Y. Zhang, L. Liu, S. Fan, Y. Wei, J. He, Controlled synthesis and field emission properties of ZnO nanostructures with different morphologies, J. Nanosci. Nanotechnol. 6 (2006) 787–790.
[8] X. Wang, Y. Ding, C.J. Summers, Z.L. Wang, Large-scale synthesis of six-nanometer-wide ZnO nanobelts, J. Phys. Chem. B 108 (2004) 8773–8777.
[9] Y.-R. Lin, S.-S. Yang, S.-Y. Tsai, H.-C. Hsu, S.-T. Wu, I.-C. Chen, Visible photoluminescence of ultrathin ZnO nanowire at room temperature, Cryst. Growth Des. 6 (2006) 1951–1955.
[10] J. Yang, G. Liu, J. Lu, Y. Qiu, S. Yang, Electrochemical route to the synthesis of ultrathin ZnO nanorod/nanobelt arrays on zinc substrate, Appl. Phys. Lett. 90 (2007) (Article Number 103109).
[11] M. Mamat, Z. Khusaimi, M. Musa, M. Malek, M. Rusop, Fabrication of ultraviolet photoconductive sensor using a novel aluminium-doped zinc oxide nanorod–nanoflake network thin film prepared via ultrasonic-assisted sol–gel and immersion methods, Sens. Actuators A: Phys. 171 (2011) 241–247.
[12] S.A. Morin, M.J. Bierman, J. Tong, S. Jin, Mechanism and kinetics of spontaneous nanotube growth driven by screw dislocations, Science 328 (2010) 476–480.
[13] B. Liu, H.C. Zeng, Room temperature solution synthesis of monodispersed single-crystalline ZnO nanorods and derived hierarchical nanostructures, Langmuir 20 (2004) 4196–4204.
[14] J. Qiu, X. Li, F. Zhuge, X. Gan, X. Gao, W. He, S.J. Park, H.K. Kim, Y.H. Hwang, Solution-derived 40 μm vertically aligned ZnO nanowire arrays as photoelectrodes in dye-sensitized solar cells, Nanotechnology 21 (2010) 195602.
[15] Z. Li, Y. Xiong, Y. Xie, Selected-control synthesis of ZnO nanowires and nanorods via a PEG-assisted route, Inorg. Chem. 42 (2003) 8105–8109.
[16] R.A. McBride, J.M. Kelly, D.E. McCormack, Growth of well-defined ZnO microparticles by hydroxide ion hydrolysis of zinc salts, J. Mater. Chem. 13 (2003) 1196–1201.
[17] P. Li, H. Liu, F. Xu, Y. Wei, Controllable growth of ZnO nanowhiskers by a simple solution route, Mater. Chem. Phys. 112 (2008) 393–397.
[18] J. Xie, P. Li, Y. Wang, Y. Wei, Synthesis of ZnO whiskers with different aspect ratios by a facile solution route, Phys. Status Solidi A 205 (2008) 1560–1565.
[19] J. Xie, P. Li, Y. Li, Y. Wang, Y. Wei, Morphology control of ZnO particles via aqueous solution route at low temperature, Mater. Chem. Phys. 114 (2009) 943–947.
[20] P. Li, H. Liu, B. Lu, Y. Wei, Formation mechanism of 1D ZnO nanowhiskers in aqueous solution, J. Phys. Chem. C 114 (2010) 21132–21137.
[21] M. Wang, Y. Zhou, Y. Zhang, S.H. Hahn, E.J. Kim, From $Zn(OH)_2$ to ZnO: a study on the mechanism of phase transformation, CrystEngComm 13 (2011) 6024–6026.
[22] N.J. Nicholas, G.V. Franks, W.A. Ducker, The mechanism for hydrothermal growth of zinc oxide, CrystEngComm 14 (2012) 1232–1240.
[23] W. Jia, S. Dang, H. Liu, Z. Zhang, C. Yu, X. Liu, B. Xu, Evidence of the formation mechanism of ZnO in aqueous solution, Mater. Lett., (2012).
[24] Q. Li, J. Bian, J. Sun, J. Wang, Y. Luo, K. Sun, D. Yu, Controllable growth of well-aligned ZnO nanorod arrays by low-temperature wet chemical bath deposition method, Appl. Surf. Sci. 256 (2010) 1698–1702.
[25] P. Zhdan, A. Shepelin, Z. Osipova, V. Sokolovskii, The extent of charge localization on oxygen ions and catalytic activity on solid state oxides in allylic oxidation of propylene, J. Catal. 58 (1979) 8–14.
[26] S. Sepulveda-Guzman, B. Reeja-Jayan, E. de La Rosa, A. Torres-Castro, V. Gonzalez-Gonzalez, M. Jose-Yacaman, Synthesis of assembled ZnO structures by precipitation method in aqueous media, Mater. Chem. Phys. 115 (2009) 172–178.
[27] J. Qiu, X. Li, W. He, S.-J. Park, H.-K. Kim, Y.-H. Hwang, J.-H. Lee, Y.-D. Kim, The growth mechanism and optical properties of ultralong ZnO nanorod arrays with a high aspect ratio by a preheating hydrothermal method, Nanotechnology 20 (2009) 155603.
[28] C. Xu, D. Gao, Two-Stage hydrothermal growth of long ZnO nanowires for efficient TiO_2 nanotube-based dye-sensitized solar cells, J. Phys. Chem. C 116 (2012) 7236–7241.
[29] K. Vanheusden, W. Warren, C. Seager, D. Tallant, J. Voigt, B. Gnade, Mechanisms behind green photoluminescence in ZnO phosphor powders, J. Appl. Phys. 79 (1996) 7983–7990.
[30] J. Wang, P. Liu, X. Fu, Z. Li, W. Han, X. Wang, Relationship between oxygen defects and the photocatalytic property of ZnO nanocrystals in nafion membranes, Langmuir 25 (2008) 1218–1223.